Designer gene networks: Towards fundamental cellular control

Jeff Hasty[a)] and Farren Isaacs
Center for BioDynamics and Department of Biomedical Engineering, Boston University,
44 Cummington St., Boston, Massachusetts 02215

Milos Dolnik
Department of Chemistry and Center for Complex Systems, Brandeis University,
Waltham, Massachusetts 02454

David McMillen and J. J. Collins
Center for BioDynamics and Department of Biomedical Engineering, Boston University, Boston,
Massachusetts 02215

The engineered control of cellular function through the design of synthetic genetic networks is becoming plausible. Here we show how a naturally occurring network can be used as a parts list for artificial network design, and how model formulation leads to computational and analytical approaches relevant to nonlinear dynamics and statistical physics. We first review the relevant work on synthetic gene networks, highlighting the important experimental findings with regard to genetic switches and oscillators. We then present the derivation of a deterministic model describing the temporal evolution of the concentration of protein in a single-gene network. Bistability in the steady-state protein concentration arises naturally as a consequence of autoregulatory feedback, and we focus on the hysteretic properties of the protein concentration as a function of the degradation rate. We then formulate the effect of an external noise source which interacts with the protein degradation rate. We demonstrate the utility of such a formulation by constructing a protein switch, whereby external noise pulses are used to switch the protein concentration between two values. Following the lead of earlier work, we show how the addition of a second network component can be used to construct a relaxation oscillator, whereby the system is driven around the hysteresis loop. We highlight the frequency dependence on the tunable parameter values, and discuss design plausibility. We emphasize how the model equations can be used to develop design criteria for robust oscillations, and illustrate this point with parameter plots illuminating the oscillatory regions for given parameter values. We then turn to the utilization of an intrinsic cellular process as a means of controlling the oscillations. We consider a network design which exhibits self-sustained oscillations, and discuss the driving of the oscillator in the context of synchronization. Then, as a second design, we consider a synthetic network with parameter values near, but outside, the oscillatory boundary. In this case, we show how resonance can lead to the induction of oscillations and amplification of a cellular signal. Finally, we construct a toggle switch from positive regulatory elements, and compare the switching properties for this network with those of a network constructed using negative regulation. Our results demonstrate the utility of model analysis in the construction of synthetic gene regulatory networks. © *2001 American Institute of Physics.*
[DOI: 10.1063/1.1345702]

Many fundamental cellular processes are governed by genetic programs which employ protein−DNA interactions in regulating function. Owing to recent technological advances, it is now possible to design synthetic gene regulatory networks. While the idea of utilizing synthetic networks in a therapeutic setting is still in its infancy, the stage is set for the notion of engineered cellular control at the DNA level. Theoretically, the biochemistry of the feedback loops associated with protein−DNA interactions often leads to nonlinear equations, and the tools of nonlinear analysis become invaluable. Here we utilize a naturally occurring genetic network to elucidate the construction and design possibilities for synthetic gene regulation.

Specifically, we show how the genetic circuitry of the bacteriophage λ can be used to design switching and oscillating networks, and how these networks can be coupled to cellular processes. In this work we suggest that a genetic toolbox can be developed using modular design concepts. Such advancements could be utilized in engineered approaches to the modification or evaluation of cellular processes.

I. INTRODUCTION

Remarkable progress in genomic research is leading to a complete map of the building blocks of biology. Knowledge of this map is, in turn, fueling the study of gene regulation, where proteins often regulate their own production or that of other proteins in a complex web of interactions. Post-

genomic research will likely center on the dissection and analysis of these complex dynamical interactions. While the notions of protein–DNA feedback loops and network complexity are not new,[1–12] experimental advances are inducing a resurgence of interest in the quantitative description of gene regulation.[13–25] These advances are beginning to set the stage for a *modular* description of the regulatory processes underlying basic cellular function.[13,26–30] In light of nearly three decades of parallel progress in the study of complex nonlinear and stochastic processes, the project of quantitatively describing gene regulatory networks is timely.

The concept of engineering genetic networks has roots that date back nearly half a century.[31,32] It is relatively recent, however, that experimental progress has made the design and implementation of genetic networks amenable to quantitative analysis. There are two dominant reasons for constructing synthetic networks. First, simple networks represent a first step towards logical cellular control, whereby biological processes can be manipulated or monitored at the DNA level.[33] Such control could have a significant impact on post-genomic biotechnology. From the construction of simple switches or oscillators, one can imagine the design of genetic code, or software, capable of performing increasingly elaborate functions.[34,30] A second complementary motivation for network construction is the scientific notion of reduced complexity; the inherently reductionist approach of decoupling a simple network from its native and often complex biological setting can lead to valuable information regarding evolutionary design principles.[35]

Ultimately, we envision the implementation of synthetic networks in therapeutic applications. However, such a utilization depends on concurrent progress in efforts to uncover basic genomic and interspecies information. For example, broad applicability will only arise with detailed information regarding tissue-specific promoters, proteins, and genes. Likewise, quantitative network design is contingent on a firm understanding of cellular differentiation and fundamental processes such as transcription, translation, and protein metabolism. More crucially, delivery is a major hurdle; without identifiable cell-specific recognition molecules, there is no method for introducing a network to a specific type of cell. Since, in many regards, therapeutic applications are somewhat premature, we focus on the implementation of synthetic networks in less complicated organisms. The design of synthetic circuits and optimization of their function in bacteria, yeast, or other plant organisms should reveal nonlinear properties that can be employed as possible mechanisms of cellular control.

In this paper, we develop several models describing the dynamics of the protein concentration in small self-contained synthetic networks, and demonstrate techniques for externally controlling the dynamics. Although our results are general, as they originate from networks designed with common gene regulatory elements, we ground the discussion by considering the genetic circuitry of bacteriophage λ. Since the range of potentially interesting behavior is wide, we focus primarily on the concentration of the λ repressor protein. We first show how bistability in the steady-state value of the repressor protein can arise from a single-gene network. We

then show how an external noise source affecting protein degradation can be introduced to our model, and how the subsequent Langevin equation is analyzed by way of transforming to an equation describing the evolution of a probability function. We then obtain the steady-state mean repressor concentration by solving this equation in the long-time limit, and discuss its relationship to the magnitude of the external perturbation. This leads to a potentially useful application, whereby one utilizes the noise to construct a genetic switch. We next show how the addition of a second network component can lead to a genetic relaxation oscillator. We study the oscillator model in detail, highlighting the essential design criteria. We introduce a mechanism for coupling the oscillator to a time-varying genetic process. In the model equations, such coupling leads to a driven oscillator, and we study the resulting system in the framework of synchronization. We illustrate the utility of such driving through the construction of an amplifier for small periodic signals. Finally, we turn to the construction of a genetic toggle switch, and compare switching times for our network with those of a network constructed using negative regulation.

II. BACKGROUND

Many processes involving cellular regulation take place at the level of gene transcription.[36,37] The very nature of cellular differentiation and role-specific interaction across cell types implicates a not yet understood order to cellular processes. Various modeling approaches have successfully described certain aspects of gene regulation in specific biological systems.[9,12–14,18,24,25,38,39] It is only recently, however, that designed network experiments have arisen in direct support of regulatory models.[21–23] In this section, we highlight the results of these experimental studies, and set the stage for the discussion of the network designs described in this work.

For completeness, we first discuss the basic concepts of promoters and regulatory feedback loops.[40,41] A *promoter region* (or, simply, a promoter) denotes a segment of DNA where a RNA polymerase molecule will bind and subsequently transcribe a gene into a mRNA molecule. Thus, one speaks of a promoter as driving the transcription of a specific gene. Transcription begins downstream from the promoter at a particular sequence of DNA that is recognized by the polymerase as the start site of transcription. A chemical sequence of DNA known as the *start codon* codes for the region of the gene that is converted into amino acids, the protein building blocks. Feedback arises when the translated protein is capable of interacting with the promoter that drives its own production or promoters of other genes. Such *transcriptional regulation* is the typical method utilized by cells in controlling expression,[42,43] and it can occur in a positive or negative sense. Positive regulation, or activation, occurs when a protein increases transcription through biochemical reactions that enhance polymerase binding at the promoter region. Negative regulation, or repression, involves the blocking of polymerase binding at the promoter region. Proteins commonly exist as multi-subunits or multimers which perform regulatory functions throughout the cell or serve as DNA-binding proteins. Typically, protein homodimers (or het-

erodimers) regulate transcription, and this fact is responsible for much of the nonlinearity that arises in genetic networks.[19]

Recently, there have been three important experimental studies involving the design of synthetic genetic networks. All three employ the use of repressive promoters. In order of increasing complexity, they consist of (i) a single autorepressive promoter utilized to demonstrate the interplay between negative feedback and internal noise,[23] (ii) two repressive promoters used to construct a genetic toggle switch,[22] and (iii) three repressive promoters employed to exhibit sustained oscillations.[21] We now briefly review the key findings in these three studies.

In the single gene study, both a negatively controlled and an unregulated promoter were utilized to study the effect of regulation on variations in cellular protein concentration.[23] The central result is that negative feedback decreases the cell-to-cell fluctuations in protein concentration measurements. Although the theoretical notion of network-induced decreased variability is not new,[44] this study empirically demonstrates the phenomenon through the measurement of protein fluorescence distributions over a population of cells. The findings show that, for a repressive network, the fluorescence distribution is significantly tightened, and that such tightening is proportional to the degree to which the promoter is negatively controlled. These results suggest that negative feedback is utilized in cellular design as a means for mitigating variations in cellular protein concentrations. Since the number of proteins per cell is typically small, internal noise is thought to be an important issue, and this study speaks to issues regarding the reliability of cellular processes in the presence of internal noise.

The toggle switch involves a network where each of two proteins negatively regulates the synthesis of the other; protein ''A'' turns off the promoter for gene ''B,'' and protein B turns off the promoter for gene A.[22] In this work, it is shown how certain biochemical parameters lead to two stable steady states, with either a high concentration of A (low B), or a high concentration of B (low A). Reliable switching between states is induced through the transient introduction of either a chemical or thermal stimulus, and shown to be significantly sharper than for that of a network designed without co-repression. Additionally, the change in fluorescence distributions during the switching process suggests interesting statistical properties regarding internal noise. These results demonstrate that synthetic toggle switches can be designed and utilized in a cellular environment. Co-repressive switches have long been proposed as a common regulatory theme,[45] and the synthetic toggle serves as a model system in which to study such networks.

In the oscillator study, three repressible promoters were used to construct a network capable of producing temporal oscillations in the concentrations of cellular proteins.[21] The regulatory network was designed with cyclic repressibility; protein A turns off the promoter for gene B, protein B turns off the promoter for gene C, and protein C turns off the promoter for gene A. For certain biochemical parameters, the ''repressilator'' was shown to exhibit self-sustained oscillations over the entire growth phase of the host E. coli cells. Interestingly, the period of the oscillations was shown to be longer than the bacterial septation period, suggesting that cellular conditions important to the oscillator network were reliably transmitted to the progeny cells. However, significant variations in oscillatory phases and amplitudes were observed between daughter cells, and internal noise was proposed as a plausible decorrelation mechanism. These variations suggest that, in order to circumvent the effects of noise, naturally-occurring oscillators might need some additional form of control. Indeed, an important aspect of this study was its focus on the utilization of synthetic networks as tools for biological inference. In this regard, the repressilator work provides potentially valuable information pertaining to the design principles of other oscillatory systems, such as circadian clocks.

These studies represent important advances in the engineering-based methodology of synthetic network design. In all three, the experimental behavior is consistent with predictions which arise from continuum dynamical modeling. Further, theoretical models were utilized to determine design criteria, lending support to the notion of an engineering-based approach to genetic network design. These criteria included the use of strong constitutive promoters, effective transcriptional repression, cooperative protein interactions, and similar protein degradation rates. In the immediate future, the construction and analysis of a circuit containing an activating control element (i.e., a positive feedback system) appears to be a next logical step.

In this work, we present several models describing the design of synthetic networks in prokaryotic organisms. Specifically, we will utilize genetic components from the virus bacteriophage λ. While other quantitative studies have concentrated on the switching properties of the λ phage circuitry,[9,12,18,38] we focus on its value as a parts list for designing synthetic networks. Importantly, the biochemical reactions that constitute the control of λ phage are very well characterized; the fundamental biochemical reactions are understood, and the equilibrium association constants are known.[9,46–50] In its naturally-occurring state, λ phage infects the bacteria Escherichia coli (E. coli). Upon infection, the evolution of λ phage proceeds down one of two pathways. The lysis pathway entails the viral destruction of the host, creating hundreds of phage progeny in the process. These progeny can then infect other bacteria. The lysogenous pathway involves the incorporation of the phage DNA into the host genome. In this state, the virus is able to dormantly pass on its DNA through the bacterial progeny. The extensive interest in λ phage lies in its ability to perform a remarkable trick; if an E. coli cell infected with a lysogen is endangered (i.e., exposure to UV radiation), the lysogen will quickly switch to the lytic pathway and abandon the challenged host cell.

The biochemistry of the viral ''abandon-ship'' response is a textbook example[36] of cellular regulation via a naturally-occurring genetic switch. The lytic and lysogenic states are controlled by the cro and cI genes, respectively. These genes are regulated by what are known as the P_{RM} (cI gene) and P_R (cro gene) promoters. They overlap in an operator region consisting of the three binding sites OR1, OR2, and OR3, and the Cro and λ repressor (''repressor,'' the cI product)

protein actively compete for these binding sites. When the Cro protein (the product of the *cro* gene) binds to these sites, it induces lysis. When repressor binds, lysogeny is maintained and lysis suppressed. When potentially fatal DNA damage is sensed by an *E. coli* host, part of the cellular response is to attempt DNA repair through the activation of a protein called RecA. λ phage has evolved to utilize RecA as a signal; RecA degrades the viral repressor protein and Cro subsequently assumes control of the promoter region. Once Cro is in control, lysis ensues and the switch is thrown.

III. BISTABILITY IN A SINGLE-GENE NETWORK

In this section, we develop a quantitative model describing the regulation of the P_{RM} operator region of λ phage. We envision that our system is a DNA plasmid consisting of the promoter region and *cI* gene.

As noted above, the promoter region contains the three operator sites known as OR1, OR2, and OR3. The basic dynamical properties of this network, along with a categorization of the biochemical reactions, are as follows. The gene *cI* expresses repressor (CI), which in turn dimerizes and binds to the DNA as a transcription factor. This binding can take place at one of the three binding sites OR1, OR2, or OR3. The binding affinities are such that, typically, binding proceeds sequentially; the dimer first binds to the OR1 site, then OR2, and last OR3.[37] Positive feedback arises due to the fact that downstream transcription is enhanced by binding at OR2, while binding at OR3 represses transcription, effectively turning off production and thereby constituting a negative feedback loop.

The chemical reactions describing the network are naturally divided into two categories—fast and slow. The fast reactions have rate constants of order seconds, and are therefore assumed to be in equilibrium with respect to the slow reactions, which are described by rates of order minutes. If we let X, X_2, and D denote the repressor, repressor dimer, and DNA promoter site, respectively, then we may write the equilibrium reactions

$$X+X \underset{}{\overset{K_1}{\rightleftharpoons}} X_2,$$

$$D+X_2 \underset{}{\overset{K_2}{\rightleftharpoons}} D_1,$$

$$D_1+X_2 \underset{}{\overset{K_3}{\rightleftharpoons}} D_2D_1, \tag{1}$$

$$D_2D_1+X_2 \underset{}{\overset{K_4}{\rightleftharpoons}} D_3D_2D_1,$$
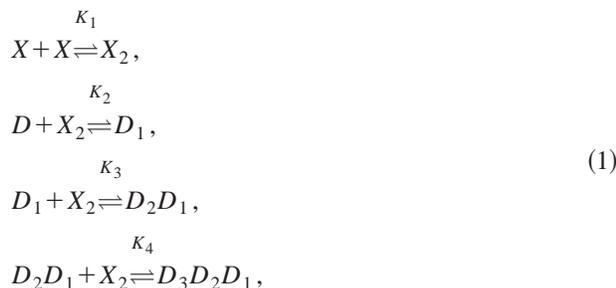
where D_i denotes dimer binding to the OR*i* site, and the $K_i=k_i/k_{-i}$ are equilibrium constants. We let $K_3=\sigma_1 K_2$ and $K_4=\sigma_2 K_2$, so that σ_1 and σ_2 represent binding strengths relative to the dimer–OR1 strength.

The slow irreversible reactions are transcription and degradation. If no repressor is bound to the operator region, or if a single repressor dimer is bound to OR1, transcription proceeds at a normal unenhanced rate. If, however, a repressor dimer is bound to OR2, the binding affinity of RNA polymerase to the promoter region is enhanced, leading to an amplification of transcription. Degradation is essentially due to cell growth. We write the reactions governing these processes as

$$D+P \overset{k_t}{\rightarrow} D+P+nX,$$

$$D_1+P \overset{k_t}{\rightarrow} D_1+P+nX,$$

$$D_2D_1+P \overset{\alpha k_t}{\rightarrow} D_2D_1+P+nX, \tag{2}$$

$$X \overset{k_x}{\rightarrow},$$
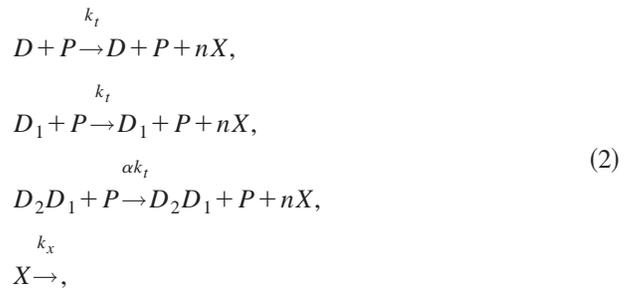
where P denotes the concentration of RNA polymerase, n is the number of repressor proteins per mRNA transcript, and $\alpha>1$ is the degree to which transcription is enhanced by dimer occupation of OR2.

Defining concentrations as our dynamical variables, $x=[X]$, $x_2=[X_2]$, $d_0=[D]$, $d_1=[D_1]$, $d_2=[D_2D_1]$, and $d_3=[D_3D_2D_1]$, we can write a rate equation describing the evolution of the concentration of repressor,

$$\dot{x}=-2k_1x^2+2k_{-1}x_2+nk_tp_0(d_0+d_1+\alpha d_2)-k_xx, \tag{3}$$

where we assume that the concentration of RNA polymerase p_0 remains constant during time.

We next eliminate x_2 and the d_i from Eq. (3) as follows. We utilize the fact that the reactions in Eq. (1) are fast compared to expression and degradation, and write algebraic expressions,

$$x_2=K_1x^2,$$

$$d_1=K_2d_0x_2=(K_1K_2)d_0x^2,$$

$$d_2=K_3d_1x_2=\sigma_1(K_1K_2)^2d_0x^4, \tag{4}$$

$$d_3=K_4d_2x_2=\sigma_1\sigma_2(K_1K_2)^3d_0x^6.$$

Further, the total concentration of DNA promoter sites d_T is constant, so that

$$md_T=d_0(1+K_1K_2x^2+\sigma_1(K_1K_2)^2x^4$$
$$+\sigma_1\sigma_2(K_1K_2)^3x^6), \tag{5}$$

where m is the copy number for the plasmid, i.e., the number of plasmids per cell.

We next eliminate two of the parameters by rescaling the repressor concentration x and time. To this end, we define the dimensionless variables $\tilde{x}=x\sqrt{K_1K_2}$ and $\tilde{t}=t(k_tp_0d_Tn\sqrt{K_1K_2})$. Upon substitution into Eq. (3), we obtain

$$\dot{x}=\frac{m(1+x^2+\alpha\sigma_1x^4)}{1+x^2+\sigma_1x^4+\sigma_1\sigma_2x^6}-\gamma_x x, \tag{6}$$

where $\gamma_x=k_x/(d_Tnk_tp_0\sqrt{K_1K_2})$, the time derivative is with respect to $\tilde{t}$, and we have suppressed the overbar on x. The equilibrium constants are $K_1=5.0\times10^7\,\text{M}^{-1}$ and $K_2=3.3\times10^8\,\text{M}^{-1}$,[9,46,48,49] so that the transformation from the dimensionless variable x to the total concentration of repressor (monomeric and dimeric forms) is given by $[\text{CI}]=(7.7x+3.0x^2)$ nM. The scaling of time involves the parameter k_t,

and since transcription and translation are actually a complex sequence of reactions, it is difficult to give this lump parameter a numerical value. However, in Ref. 51, it is shown that, by utilizing a model for the lysogenous state of the λ phage, a consistency argument yields a value for the product of parameters $(d_t n k_t p_0) = 87.6$ nM min^{-1}. This leads to a transformation from the dimensionless time $\tilde{t}$ to time measured in minutes of $t(\text{min}) = 0.089\tilde{t}$.

Since equations similar to Eq. (3) often arise in the modeling of genetic circuits (see Refs. 52 of this Focus Issue), it is worth noting the specifics of its functional form. The first term on the right hand side of Eq. (6) represents production of repressor due to transcription. The even polynomials in x occur due to dimerization and subsequent binding to the promoter region. As noted above, the σ_i prefactors denote the relative affinities for dimer binding to OR1 versus that of binding to OR2 (σ_1) and OR3 (σ_2). The prefactor $\alpha > 1$ on the x^4 term is present because transcription is enhanced when the two operator sites OR1 and OR2 are occupied ($x^2 x^2$). The x^6 term represents the occupation of all three operator sites, and arises in the denominator because dimer occupation of OR3 inhibits polymerase binding and shuts off transcription.

For the operator region of λ phage, we have $\sigma_1 \sim 2$, $\sigma_2 \sim 0.08$, and $\alpha \sim 11$,[9,46,48,49] so that the parameters γ_x and m in Eq. (6) determine the steady-state concentration of repressor. The parameter γ_x is directly proportional to the protein degradation rate, and in the construction of artificial networks, it can be utilized as a tunable parameter. The integer parameter m represents the number of plasmids per cell. While this parameter is not accessible during an experiment, it is possible to design a plasmid with a given copy number, with typical values in the range of 1–100.

The nonlinearity of Eq. (6) leads to a bistable regime in the steady-state concentration of repressor, and in Fig. 1(a) we plot the steady-state concentration of the repressor as a function of the parameter γ_x. The bistability arises as a consequence of the competition between the production of x along with dimerization and its degradation. For certain parameter values, the initial concentration is irrelevant, but for those that more closely balance production and loss, the final concentration is determined by the initial value.

Before turning to the next section, we make one additional observation regarding the synonymous issues of the general applicability of a synthetic network and experimental measurement. In experimental situations, a Green Fluorescent Protein (GFP) is often employed as a measurement tag known as a reporter gene. This is done by inserting the gene encoding GFP adjacent to the gene of interest, so that the reporter protein is produced in tandem with the protein of interest. In the context of the formulation given above, we can generalize Eq. (6) to include the dynamics of the reporter protein,

$$\dot{x} = f(x) - \gamma_x x,$$

$$\dot{g} = f(x) - \gamma_g g, \tag{7}$$

where $f(x)$ is the nonlinear term in Eq. (6), $\gamma_g = k_g/(d_T n k_t p_0 \sqrt{K_1 K_2})$, and the GFP concentration is scaled
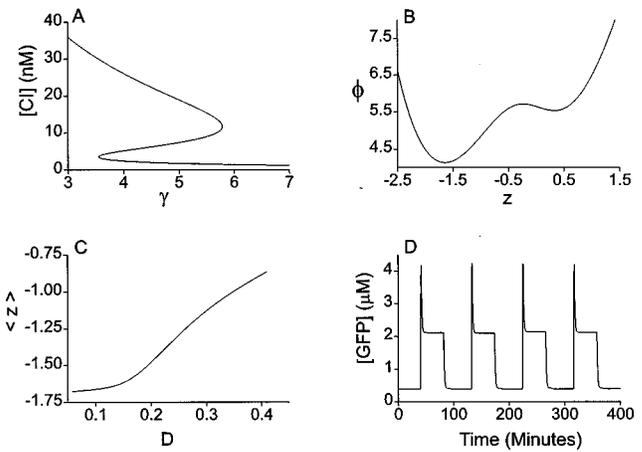
FIG. 1. Results for additive noise with parameter value $m = 1$. (a) Bifurcation plot for the steady-state concentration of repressor vs the model parameter γ_x. (b) The energy landscape. Stable equilibrium values of Eq. (10) (with $D = 0$) correspond to the valleys at $z = -1.6$ and 0.5, with an unstable value at $z = -0.52$. (b) Steady-state probability distributions for noise strengths of $D = 0.04$ (solid line) and $D = 0.4$ (dotted line). (c) The steady-state equilibrium value of z plotted vs noise strength. The corresponding concentration will increase as the noise causes the upper state of (b) to become increasingly populated. (d) The simulation of Eqs. (8) and (9) demonstrating the utilization of external noise for protein switching. Initially, the concentration begins at a level of $[\text{GFP}] \sim 0.4$ μM corresponding to a low noise value of $D = 0.01$. After 40 minutes, a large 2-minute noise pulse of strength $D = 1.0$ is used to drive the concentration to ~ 2.2 μM. Following this pulse, the noise is returned to its original value. At 80 minutes, a smaller 10-minute noise pulse of strength $D = 0.1$ is used to return the concentration to near its original value. The simulation technique is that of Ref. 53.

by the same factor as repressor ($\tilde{g} = g \sqrt{K_1 K_2}$). In analogy with the equation for x, k_g is the degradation rate for GFP, and we have assumed that the number of proteins per transcript n is the same for both processes. This ability to co-transcribe two genes from the same promoter and transcribe in tandem has two important consequences. First, since proteins are typically very stable, it is often desirable to substantially increase their degradation rate in order to access some nonlinear regime.[21,22] Such a high degradation rate typically will lead to a low protein concentration, and this, in turn, can induce detection problems. The utilization of a GFP-type reporter protein can help to mitigate this problem, since its degradation rate can be left at a relatively low value. Second, and perhaps more importantly, are the significant implications for the generality of designer networks; in prokaryotic organisms, *any* protein can be substituted for GFP and co-transcribed, so that one network design can be utilized in a myriad of situations.

IV. A NOISE-BASED PROTEIN SWITCH

We now focus on parameter values leading to bistability, and consider how an external noise source can be utilized to alter the production of protein. Physically, we take the dynamical variables x and g described above to represent the protein concentrations within a colony of cells, and consider the noise to act on many copies of this colony. In the absence of noise, each colony will evolve identically to one of the two fixed points, as discussed above. The presence of a noise

source will at times modify this simple behavior, whereby colony-to-colony fluctuations can induce novel behavior.

Noise in the form of random fluctuations arises in biochemical networks in one of two ways. As discussed elsewhere in this Focus Issue,[54] *internal* noise is inherent in biochemical reactions, often arising due to the relatively small numbers of reactant molecules. On the other hand, *external* noise originates in the random variation of one or more of the externally-set control parameters, such as the rate constants associated with a given set of reactions. If the noise source is small, its effect can often be incorporated *post hoc* into the rate equations. In the case of internal noise, this is done in an attempt to recapture the lost information embodied in the rate-equation approximation. But in the case of external noise, one often wishes to introduce some new phenomenon where the details of the effect are not precisely known. In either case, the governing rate equations are augmented with additive or multiplicative stochastic terms. These terms, viewed as a random perturbation to the deterministic picture, can induce various effects, most notably, switching between potential attractors (i.e., fixed points, limit cycles, chaotic attractors).[55]

In previous work, the effects of coupling between an external noise source and both the basal production rate and the transcriptional enhancement process were examined.[56] Here, we analyze the effect of a noise source which alters protein degradation. Since the mathematical formulation is similar to that of Ref. 56, our goal here is to reproduce the phenomenology of that work under different assumptions. As in Ref. 56, we posit that the external noise effect will be small and can be treated as a random perturbation to our existing treatment; we envision that events induced will be interactions between the external noise source and the protein degradation rate, and that this will translate to a rapidly varying protein degradation embodied in the external parameters γ_x and γ_g. In order to introduce this effect, we generalize the model of the previous section such that random fluctuations enter Eq. (7) multiplicatively,

$$\dot{x} = f(x) - (\gamma_x - \xi_x(t))x, \tag{8}$$

$$\dot{g} = f(x) - (\gamma_g - \xi_g(t))g, \tag{9}$$

where the $\xi_i(t)$ are rapidly fluctuating random terms with zero mean ($\langle \xi_i(t) \rangle = 0$). In order to encapsulate the independent random fluctuations, we make the standard requirement that the autocorrelation be "δ-correlated," i.e., the statistics of the $\xi_i(t)$ are such that $\langle \xi_i(t)\xi_j(t') \rangle = D\delta_{i,j}(t-t')$, with D proportional to the strength of the perturbation, and we have assumed that the size of the induced fluctuations is the same for both proteins.

Since, in Eqs. (8) and (9), the reporter protein concentration g does not couple to the equation for the repressor concentration, the qualitative behavior of the set of equations may be obtained by analyzing x. We first define a change of variables which transforms the multiplicative Langevin equation to an additive one. Letting $x = e^z$, Eq. (8) becomes

$$\dot{z} = \frac{1 + e^{2z} + 22e^{4z}}{e^z + e^{3z} + 2e^{5z} + .16e^{7z}} - \gamma_x + \xi_x(t) \equiv g(z) + \xi_x(t). \tag{10}$$

Equation (10) can be rewritten as

$$\dot{z} = -\frac{\partial \phi(z)}{\partial z} + \xi_x(t) \tag{11}$$

where the potential $\phi(z)$ is introduced:

$$\phi(z) = -\int g(z)dz; \tag{12}$$

$\phi(z)$ can be viewed as an ''energy landscape,'' whereby z is considered the position of a particle moving in the landscape. One such landscape is plotted in Fig. 1(b). Note that the stable fixed points correspond to the minima of the potential ϕ in Fig. 1(b), and the effect of the additive noise term is to cause random kicks to the particle (system state point) lying in one of these minima. On occasion, a sequence of kicks may enable the particle to escape a local minimum and reside in a new valley.

In order to analyze Eq. (11), one typically introduces the probability distribution $P(z,t)$, which is effectively the probability of finding the system in a state z at time t. Then, given Eq. (11), a Fokker–Planck equation for $P(z,t)$ can be constructed.[57] The steady-state solution for this equation is given by

$$P_s(z) = Ae^{-(2/D)\,\phi(z)}, \tag{13}$$

where A is a normalization constant determined by requiring the integral of $P_s(z)$ over all z be unity.

Using the steady-state distribution, the steady-state mean (ssm), $\langle z \rangle_{ss}$, is given by

$$\langle z \rangle_{ss} = \int_0^\infty zAe^{-(2/D)\,\phi(z)}dz. \tag{14}$$

In Fig. 1(c), we plot the ssm value of z as a function of D, obtained by numerically integrating Eq. (14). It can be seen that the ssm of z increases with D, corresponding to the increasing likelihood of populating the upper state in Fig. 1(b).

Figure 1(c) indicates that the external noise can be used to control the ssm concentration. As a candidate application, consider the following protein switch. Given parameter values leading to the landscape of Fig. 1(b), we begin the switch in the ''off'' position by tuning the noise strength to a very low value. This will cause a high population in the lower state, and a correspondingly low value of the concentration. Then at some time later, consider pulsing the system by increasing the noise to some large value for a short period of time, followed by a decrease back to the original low value. The pulse will cause the upper state to become populated, corresponding to a concentration increase and a flipping of the switch to the ''on'' position. As the pulse quickly subsides, the upper state remains populated as the noise is not of sufficient strength to drive the system across either barrier (on relevant time scales). To return the switch to the off position, the upper-state population needs to be decreased to a low value. This can be achieved by applying a second

A

B
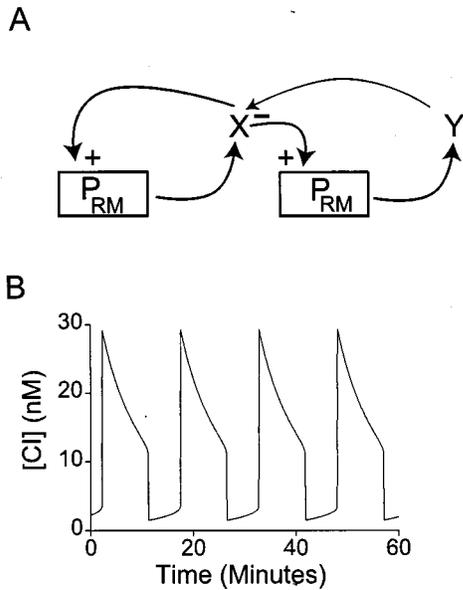
FIG. 2. The relaxation oscillator. (a) Schematic of the circuit. The P_{RM} promoter is used on two plasmids to control the production of repressor (X) and RcsA (Y). After dimerization, the repressor acts to turn on both plasmids through its interaction at P_{RM}. As its promoter is activated, RcsA concentrations rise, leading to an induced reduction of the repressor. (b) The simulation of Eqs. (15). Oscillations arise as the RcsA-induced degradation of repressor causes a transversal of the hysteresis diagram in Fig. 1(a). The parameter values are $m_x = 10$, $m_y = 1$, $\gamma_x = 0.1$, $\gamma_y = 0.01$, and $\gamma_{xy} = 0.1$.

noise pulse of intermediate strength. This intermediate value is chosen large enough so as to enhance transitions to the lower state, but small enough as to remain prohibitive to upper-state transitions.

Figure 1(d) depicts the time evolution of the switching process for noise pulses of strengths $D = 1.0$ and $D = 0.1$. Initially, the concentration begins at a level of ~ 0.4 μM, corresponding to a low noise value of $D = 0.01$. At 40 minutes, a noise burst of strength $D = 1.0$ is used to drive the concentration to a value of ~ 2.2 μM. Following this burst, the noise is returned to its original value. At 80 minutes, a second noise burst of strength $D = 0.1$ is used to return concentration to its original value.

V. A GENETIC RELAXATION OSCILLATOR

The repressillator represents an impressive step towards the generation of controllable *in vivo* genetic oscillations. However, there were significant cell-to-cell variations, apparently arising from small molecule number fluctuations.[21,35] In order to circumvent such variability, the utilization of hysteresis-based oscillations has recently been proposed.[35] In this work, it was shown how a model circadian network can oscillate reliably in the presence of internal noise. In this section, we describe an implementation of such an oscillator, based on the repressor network of Sec. III.

The hysteretic effect in Fig. 1(a) can be employed to induce oscillations, provided we can couple the network to a slow subsystem that effectively drives the parameter γ_x. This can be done by inserting a repressor protease under the control of a separate P_{RM} promoter region. The network is depicted in Fig. 2(a). On one plasmid, we have the network

of Sec. III; the repressor protein CI, which is under the control of the promoter P_{RM}, stimulates its own production at low concentrations and shuts off the promoter at high concentrations. On a second plasmid, we again utilize the P_{RM} promoter region, but here we insert the gene encoding the protein RcsA. The crucial interaction is between RcsA and CI; RcsA is a protease for repressor, effectively inactivating its ability to control the P_{RM} promoter region.[58]

The equations governing this network can be deduced from Eq. (6) by noting the following. First, both RcsA and repressor are under the control of the same promoter, so that the functional form of the production term $f(x)$ in Eq. (6) will be the same for both proteins. Second, we envision our network as being constructed from two plasmids—one for the repressor and one for RcsA, and that we have control over the number of plasmids per cell (copy number) of each type. Last, the interaction of the RcsA and repressor proteins leads to the degradation of the repressor. Putting these facts together, and letting y denote the concentration of RcsA, we have

$$\dot{x} = m_x f(x) - \gamma_x x - \gamma_{xy} x y$$

$$= m_x f(x) - \gamma(y)x, \tag{15}$$

$$\dot{y} = m_y f(x) - \gamma_y y,$$

where $\gamma(y) \equiv \gamma_x + \gamma_{xy} y$, and m_x and m_y denote the plasmid copy numbers for the two species.

In Fig. 2(b), we present simulation results for the concentration of repressor as a function of time. The nature of the oscillations can be understood using Fig. 1(a). Suppose we begin with a parameter value of $\gamma(y) = 4$ on the upper branch of the figure. The large value of the repressor will then serve to activate the promoter for the RcsA, and thus lead to its increased production. An increase in the RcsA acts as an additive degradation term for the repressor [see Eq. (15)], and thus effectively induces slow motion to the right on the upper branch of Fig. 1(a). This motion will continue until the repressor concentration falls off the upper branch at $\gamma(y) \sim 5.8$. At this point, with the repressor concentration at a very low value, the promoters are essentially turned off. Then, as RcsA begins to degrade, the repressor concentration slowly moves to left along the lower branch of Fig. 1(a), until it encounters the bifurcation point at $\gamma(y) \sim 3.6$. It then jumps to its original high value, with the entire process repeating and producing the oscillations in Fig. 2(b).

The oscillations in Fig. 2(b) are for specific parameter values; of course, not all choices of parameters will lead to oscillations. The clarification of the specific parameter values leading to oscillations is therefore important in the design of synthetic networks.[21] For proteins in their native state, the degradation rates γ_x and γ_y are very small, corresponding to the high degree of stability for most proteins. For example, a consistency argument applied to a similar model for λ phage switching[51] leads to $\gamma_x \sim 0.004$. However, using a temperature-sensitive variety of the repressor protein, γ_x can be made tunable over many orders of magnitude. Other techniques, such as SSRA tagging or titration, can be employed to increase the degradation rate for RcsA. The copy numbers
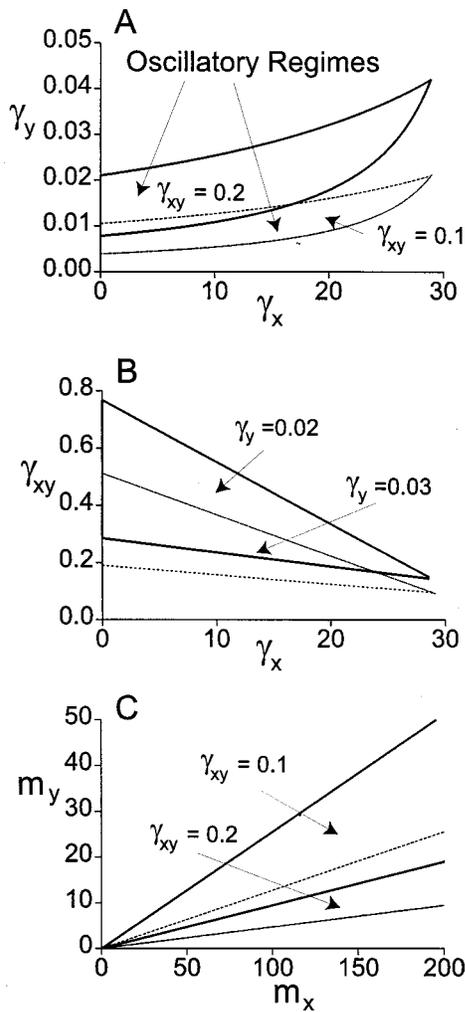
FIG. 3. Oscillatory regimes for the relaxation oscillator. (a) The bifurcation wedge is larger for smaller values of the parameter γ_{xy}. This larger regime corresponds to larger values of the RcsA degradation parameter γ_y. Note that the native (i.e., without tuning) degradation rates of $\gamma_x \sim \gamma_y \sim 0.005$ are very near the oscillatory regime. (b) Bifurcation diagrams as a function of γ_x and γ_{xy}, and for two fixed values of γ_y. The oscillatory regime is increased for smaller values of γ_y, and, in both cases, small values of γ_x are preferable for oscillations. (c) The bifurcation diagram as a function of the copy numbers m_x and m_y, and for fixed degradation rates. Importantly, one can adjust the periodic regime to account for the unknown parameter γ_{xy}. The figure also indicates that, for oscillations, one should choose as large a copy number as possible for the plasmid containing the repressor protein (m_x). In (a) and (b), constant parameter values are $m_x = 10$ and $m_y = 1$, and in (c) $\gamma_x = 1.0$ and $\gamma_y = 0.01$.

m_x and m_y can be chosen for a particular design, and the parameter γ_{xy}, which measures the rate of repressor degradation by RcsA, is unknown.

In Fig. 3(a), we present oscillatory regimes for Eq. (15) as a function of γ_x and γ_y, and for two fixed values of the parameter γ_{xy}. We see that the oscillatory regime is larger for smaller values of the parameter γ_{xy}. However, the larger regime corresponds to larger values of the degradation rate for RcsA. Interestingly, if we take the native (i.e., without tuning) degradation rates to be $\gamma_x \sim \gamma_y \sim 0.005$, we note that the system is naturally poised very near the oscillatory regime. In Fig. 3(b), we present the oscillatory regime as a function of γ_x and γ_{xy}, and for two fixed values of γ_y. The
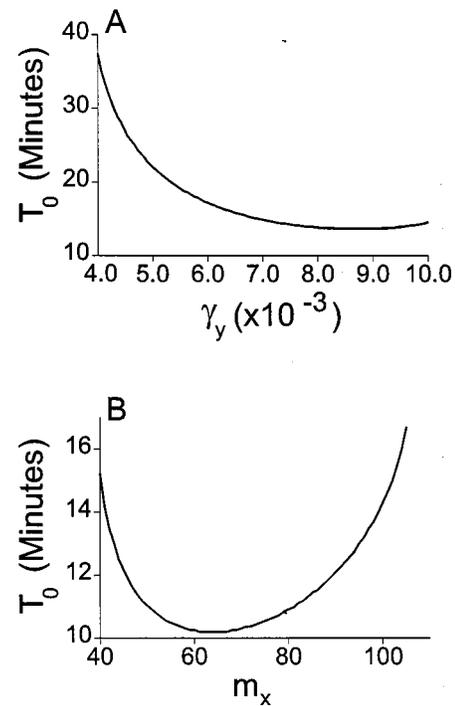
FIG. 4. Parameter dependence of the oscillatory period. (a) An increase in γ_y decreases the period of oscillations. (b) The period depends very weakly on the copy number. In (a) $m_x = 10$ and in (b) $\gamma_y = 0.01$, and for both plots, other parameter values are $\gamma_x = 0.1$, $\gamma_x y = 0.1$, and $m_y = 1$.

regime is increased for smaller values of γ_y, and, in both cases, small values of γ_x are preferable. Moreover, both Figs. 3(a) and 3(b) indicate that the system will oscillate for *arbitrarily* small values of the repressor degradation parameter γ_x. In Fig. 3(c) we depict the oscillatory regime as a function of the copy numbers m_x and m_y, and for fixed degradation rates. Importantly, one can adjust the periodic regime to account for the unknown parameter γ_{xy}. Figure 3(c) indicates that, for oscillations, one should choose as large a copy number as possible for the plasmid containing the repressor protein (m_x). Correspondingly, one should design the RcsA plasmid with a significantly smaller copy number m_y.

We now turn briefly to the period of the oscillations. If designed genetic oscillations are to be utilized, an important issue is the dependence of the oscillation period on the parameter values. In Fig. 4(a) we plot the oscillation period for our CI-RcsA network as a function of the degradation parameter γ_y, and for other parameter values corresponding to the lower wedge of Fig. 3(a). We observe that an increase in γ_y will decrease the period of oscillations. Further, since the cell-division period for *E. coli* is $\sim 35-40$ minutes, we note that the lower limit roughly corresponds to this period, and that, at the upper limit, we can expect four oscillations per cell division. The utilization of tuning the period of the oscillations to the cell-division time will be discussed in the next section. In Fig. 4(b), we plot the period as a function of the copy number m_x. We observe that the period depends very weakly on the copy number.

VI. DRIVING THE OSCILLATOR

We next turn to the utilization of an intrinsic cellular process as a means of controlling the oscillations described in the previous section. We will first consider a network design which exhibits self-sustained oscillations (i.e., with parameters that are in one of the oscillatory regions of Fig. 3), and discuss the driving of the oscillator in the context of synchronization. As a second design, we will consider a synthetic network with parameter values near, but outside, the oscillatory boundary. In that case, we will show how resonance can lead to the induction of oscillations and amplification of a cellular signal.

We suppose that an intrinsic cellular process involves oscillations in the production of protein U, and that the concentration of U is given by $u = u_0 \sin \omega t$. In order to couple the oscillations of U to our network, we imagine inserting the gene encoding repressor adjacent to the gene encoding U. Then, since U is being transcribed periodically, the co-transcription of repressor will lead to an oscillating source term in Eq. (15),

$$\dot{x} = m_x f(x) - \gamma_x x - \gamma_{xy} xy + \Gamma \sin(\omega t),$$
$$\dot{y} = m_y f(x) - \gamma_y y. \tag{16}$$

We first consider parameter values as in Fig. 2, so that the concentrations x and y oscillate in the absence of driving. Here, we are interested in how the drive affects the "internal" oscillations. Although there are many interesting properties associated with driven nonlinear equations such as Eq. (16), we focus on the conditions whereby the periodic drive can cause the dynamics to shift the internal frequency and entrain to the external drive frequency ω. We utilize the numerical bifurcation and continuation package CONT[59] to determine the boundaries of the major resonance regions. These boundaries are depicted in the parameter-space plot of Fig. 5(a), where the period of the drive is plotted versus the drive amplitude. The resonance regions form the so-called Arnold tongues, which display an increasing range of the locking period as the amplitude of drive is increased. Without the periodic drive, the period of the autonomous oscillations is equal to 14.6 minutes. As one might expect, the dominant Arnold tongue is found around this autonomous period. Within this resonance region, the period of the oscillations is entrained, and is equal to the external periodic force. The second largest region of frequency locking occurs for periods of forcing which are close to half of the period of the autonomous oscillations. As a result of the periodic driving, we observe 1:2 locking, whereby the system responds with one oscillatory cycle, while the drive has undergone two cycles. Other depicted resonant regions (3:2, 2:1, 5:2, 3:1) display significantly narrower ranges for locking periods. This suggests that higher order frequency locking will be less common and probably unstable in the presence of noise. Outside the resonance regions shown in Fig. 5(a) one can find a rich structure of very narrow $M:N$ locking regions with M and N quite large, together with quasiperiodic oscillations. The order of resonances along the drive period axis is given by the Farey sequence,[60] i.e., in between two reso-
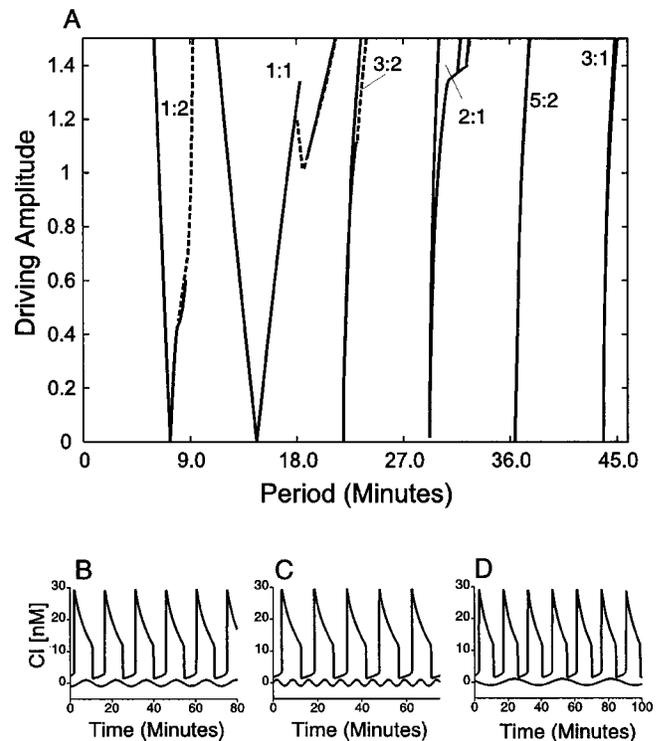
FIG. 5. Dynamics of a periodically driven relaxation oscillator—Eq. (15); $\gamma_x = 0.1$, $\gamma_y = 0.01$, $\gamma_{xy} = 0.1$. (a) Resonant regions in a period–amplitude parametric plane. Solid lines (limit lines of periodic solutions) together with dashed (period doubling) lines define boundaries of stable periodic solutions for a given phase locking region $M:N$, where M is the number of relaxation oscillation and N is the number of driving sinusoidal oscillations. (b–d) Oscillations in a periodically driven repressor (top curve) concentration together with the oscillations of the sinusoidal driving (bottom curve). (b) 1:1 synchronization; the 14.6 minute period of cI oscillations is equal to the driving period. (c) 1:2 phase locking; the 29.2 minute period of the cI oscillations is twice as long as the driving period. (d) 2:1 phase locking; the 7.6 minute period of the cI oscillations is equal to one half of the driving period.

nance regions characterized by rational numbers, $M_1:N_1$ and $M_2:N_2$, there is a region with ratio $(M_1 + M_2):(N_1 + N_2)$.

The preceding notions correspond to the driving of genetic networks which are intrinsically oscillating. We now turn to a network designed with parameter values just outside the oscillatory region, and consider the use of resonance in the following application. Suppose there is a cellular process that depends critically on oscillations of a given amplitude. We seek a strategy for modifying the amplitude of this process if, for some reason, it is too small. For concreteness, consider a cellular process linked to the cell-division period of the host for our synthetic network. For $E.$ $coli$ cells at a temperature of $\sim 37\,°C$, this period is of order 35–40 minutes. Using Figs. 3(a) and 4(a), we can deduce parameter values that will cause a CI-RscA network to oscillate, when driven, with this period. The lower wedge of Fig. 3(a) implies that, for $\gamma_{xy} = 0.1$, we should design the network with values of γ_x and γ_y just below the lower boundary of the wedge. Figure 4(a) implies that, for $\gamma_x = 0.1$, a choice of $\gamma_y = 0.004$ will yield oscillations with a period close to the cell-division period. In order to stay outside the oscillatory region, we therefore choose γ_y just below this value. Taken together, these choices will yield a network whereby oscilla-
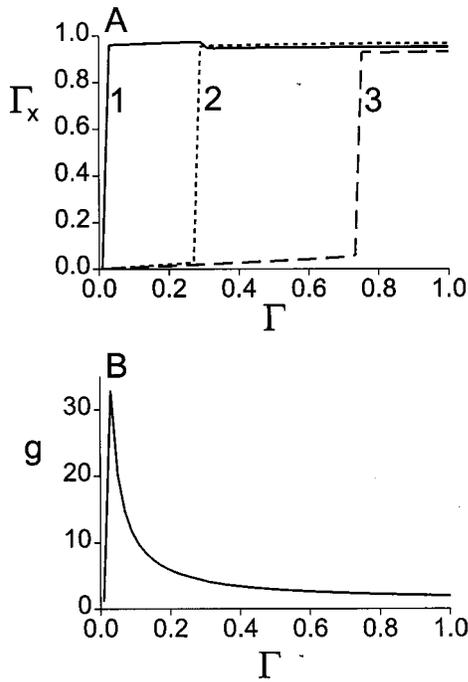
FIG. 6. (a) As a function of the driving amplitude Γ, the amplitude Γ_x of the induced network oscillations shows a sharp increase for a critical value of the drive. The critical value corresponds to a drive large enough to induce the hysteretic oscillations, and it increases as one decreases γ_y and moves away from the oscillatory region in parameter space. The three curves denoted 1, 2, and 3 are for γ_y values of 0.0038, 0.0036, and 0.0034. (b) The gain as a function of the drive amplitude for $\gamma_y = 0.0038$. Close to the oscillatory region, a significant gain in the drive amplitude can be induced. Parameter values for both plots are $\gamma_x = 0.1$, $\gamma_{xy} = 0.1$, $m_x = 10$, and $m_y = 1$. Note that, corresponding to these values, the network does not oscillate (without driving) for $\gamma_y < 0.004$ [see the bottom wedge of Fig. 3(a)].

tions can be induced by cellular processes related to cell division. In Fig. 6(a), we plot the drive versus response amplitudes (Γ vs Γ_x) obtained from the numerical integration of Eq. (16). We see that, depending on the proximity to the oscillatory region, oscillations are triggered when the drive reaches some critical amplitude. In Fig. 6(b), we plot the gain $g \equiv (\Gamma + \Gamma_x)/\Gamma$ as a function of the drive amplitude Γ, and observe that, for certain values of the amplitude of the drive, the network can induce a significant gain.

VII. HARNESSING THE LAMBDA SWITCH

The ability to switch between multiple stable states is a critical first step towards sophisticated cellular control schemes. Nonlinearities giving rise to two stable states suggest the possibility of using these states as digital signals to be processed in cellular-level computations (see, for example, Refs. 30 and 34). One may eventually be able to produce systems in which sequences of such switching events are combined to control gene expression in complex ways. In any such application, the speed with which systems make transitions between their stable states will act as a limiting factor on the time scales at which cellular events may be controlled. In this section, we describe a bistable switch based on the mechanism used by λ phage, and show that such a system offers rapid switching times.

The genetic network of λ phage switches its host bacterium from the dormant lysogenous state to the lytic growth state in roughly twenty minutes).[61] As discussed in Sec. II, the regulatory network implementing this exceptionally fast switch has two main features: two proteins (CI and Cro) compete directly for access to promoter sites; and one of the proteins (CI) positively regulates its own level of transcription. Here, we compare a synthetic switch based on the λ phage's switching mechanism to another two-protein switch (the toggle switch described in Ref. 22), and numerically show that the λ-like system offers a faster switching time under comparable conditions.

To implement the synthetic λ switch, we use the plasmid described in Sec. III, on which the P_{RM} promoter controls the expression of the λ repressor protein, CI. To this, we add a second plasmid on which the P_R promoter is used to control the expression of Cro. The operator regions OR1, OR2, and OR3 exist on each plasmid, and both proteins are capable of binding to these regions on either of the plasmids. On the P_{RM}-promoter plasmid, transcription of CI takes place whenever there is no protein (of either type) bound to OR3; when CI is bound to OR2, the rate of CI transcription is enhanced. On the P_R-promoter plasmid, Cro is transcribed only when operator site OR3 is either clear, or has a Cro dimer bound to it; either protein being bound to either OR1 or OR2 has the effect of halting the transcription of Cro.

Letting y represent the concentration of Cro, the competition for operator sites leads to equations of the form $\dot{x} = f(x,y) - \gamma_x x$, $\dot{y} = g(x,y) - \gamma_y y$. We derive the form of these equations by following the process described in Sec. III. As with the CI plasmid of that section, we have Eq. (1) describing the equilibrium reactions for the binding of CI to the various operator sites. To these, we add the reactions entailing the binding of Cro, and the reactions in which both proteins are bound simultaneously to different operator sites:

$$Y + Y \underset{}{\overset{K_3}{\rightleftharpoons}} Y_2,$$

$$D + Y_2 \underset{}{\overset{K_4}{\rightleftharpoons}} D_3^Y,$$

$$D_3^Y + Y_2 \underset{}{\overset{\beta_1 K_4}{\rightleftharpoons}} D_3^Y D_2^Y,$$

$$D_3^Y + Y_2 \underset{}{\overset{\beta_2 K_4}{\rightleftharpoons}} D_3^Y D_1^Y,$$

$$D_3^Y D_2^Y + Y_2 \underset{}{\overset{\beta_3 K_4}{\rightleftharpoons}} D_3^Y D_2^Y D_1^Y, \tag{17}$$

$$D_2^X D_1^X + Y_2 \underset{}{\overset{\beta_4 K_4}{\rightleftharpoons}} D_3^Y D_2^X D_1^X,$$

$$D_1^X + Y_2 \underset{}{\overset{\beta_5 K_4}{\rightleftharpoons}} D_3^Y D_1^X,$$
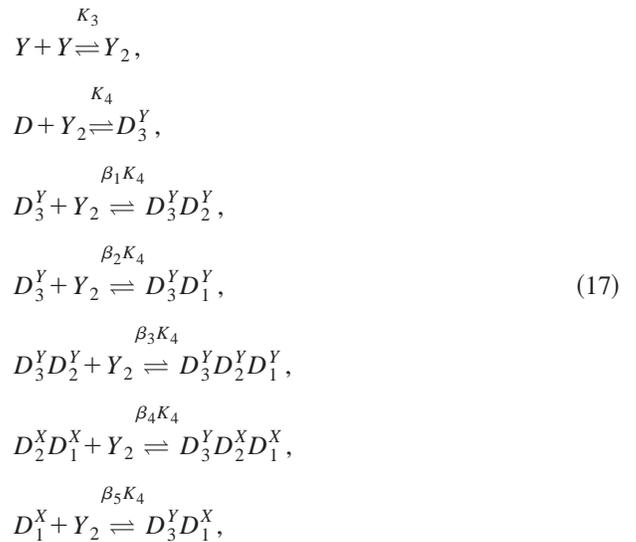
where Y represents the Cro monomer, and D_i^p represents the binding of protein p to the ORi site. For the operator region of λ phage, we have $\beta_1 \simeq \beta_2 \simeq \beta_3 \sim 0.08$, and $\beta_4 \simeq \beta_5 \sim 1$.[46,48,49]

The transcriptional processes are as follows. Transcription of repressor takes place when there is no protein (of

either type) bound to OR3. When repressor is bound to OR2, the rate of repressor transcription is enhanced, and Cro is transcribed only when OR3 is either vacant, or has a Cro dimer bound to it. If either repressor or Cro is bound to either OR1 or OR2, the production of Cro is halted. These processes, along with degradation, yield the following irreversible reactions:

$$D + P \xrightarrow{k_{tx}} D + P + n_x X,$$

$$D_1^X + P \xrightarrow{k_{tx}} D_1^X + P + n_x X,$$

$$D_2^X D_1^X + P \xrightarrow{\alpha k_{tx}} D_2^X D_1^X + P + n_x X,$$

$$D + P \xrightarrow{k_{ty}} D + P + n_y Y,$$ (18)

$$D_3^Y + P \xrightarrow{k_{ty}} D_3^Y + P + n_y Y,$$

$$X \xrightarrow{k_{dx}},$$

$$Y \xrightarrow{k_{dy}},$$
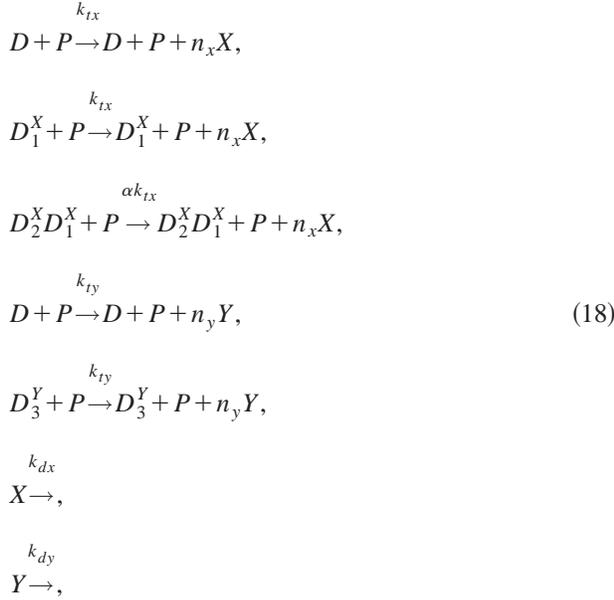
Following the rate equation formulation of Sec. III, we obtain

$$\dot{x} = \frac{m_x(1 + x^2 + \alpha\sigma_1 x^4)}{Q(x,y)} - \gamma_x x,$$
  (19)
$$\dot{y} = \frac{m_y \rho_y (1 + y^2)}{Q(x,y)} - \gamma_y y,$$

where

$$Q(x,y) = 1 + x^2 + \sigma_1 x^4 + \sigma_1 \sigma_2 x^6 + y^2 + (\beta_1 + \beta_2)y^4$$
$$+ \beta_1 \beta_3 y^6 + \sigma_1 \beta_4 x^4 y^2 + \beta_5 x^2 y^2.$$

The derivatives are with respect to dimensionless time, with scaling as in Sec. III; $\tilde{t} = t(k_{tx}p_0 d_T n_x \sqrt{K_1 K_2})$, where k_{tx} is the transcription rate constant for CI, and n_x is the number of CI monomers per mRNA transcript. The integers m_x and m_y represent the plasmid copy numbers for the two species; ρ_y is a constant related to the scaling of y relative to x. The parameters γ_x and γ_y are directly proportional to the decay rates of CI and Cro, respectively; we will tune these values to cause transitions between stable states. The system exhibits bistability over a wide range of parameter values, and we plot the null-clines in Fig. 7(a).

For comparison, we now consider the co-repressive toggle switch briefly reviewed in Sec. II.[22] This switch uses the CI and Lac proteins, where each protein shuts off transcription from the other protein's promoter region. The experimental design was guided by the model equations,
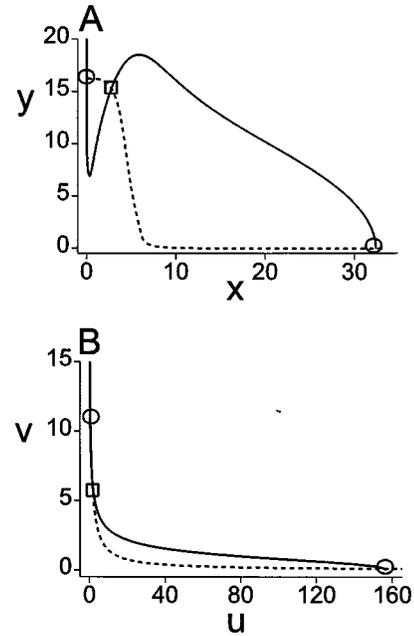
FIG. 7. Null-clines for the two-protein bistable switch systems. Stable fixed points are marked with circles, and unstable fixed points are marked with squares. (a) Null-clines for the synthetic λ switch, Eqs. (19). Solid line: $\dot{x} = 0$ cline. Dashed line: $\dot{y} = 0$ cline. Parameter values: $\gamma_x = 0.004$; $\gamma_y = 0.008$; $\rho_y = 62.92$; $\alpha = 11$; $m_x = m_y = 1$; $\sigma_1 = 2$; $\sigma_2 = 0.08$; $\beta_1 = \beta_2 = \beta_3 = 0.08$; and $\beta_4 = \beta_5 = 1$. (b) Null-clines for the toggle switch, Eqs. (20). Solid line: $\dot{u} = 0$ cline. Dashed line: $\dot{v} = 0$ cline. Parameter values (from Ref. 22): $\alpha_1 = 156.25$; $\alpha_2 = 15.6$; $\delta = 2.5$; $\mu = 1$; $\eta = 2.0015$; [IPTG]=0; $k = 1$.

$$\dot{u} = \frac{\alpha_1}{1 + v^\delta} - u,$$
  (20)
$$\dot{v} = \frac{\alpha_2}{1 + [u/(1 + /[IPTG]/K)^\eta]^\mu} - kv,$$

where u and v are dimensionless concentrations of the Lac and CI proteins, respectively, and the time derivatives are with respect to a dimensionless time: $\tau = k_d t$, with $k_d = 2.52$ h^{-1} (Refs. 12 and 18) being the protein decay rate. The dimensionless parameters α_1, α_2, δ, and μ define the basic model. The CI protein used in the experiments is temperature-sensitive, changing its rate of degradation with temperature;[62,63] we modify the original model slightly to include the factor k, which represents a varying decay rate for the CI protein. Switching is induced by changing k, or by adjusting the concentration of isopropyl-β-D-thiogalacto-pyranoside (IPTG); the parameters $K = 2.9618 \times 10^{-5}$ M and $\eta = 2.0015$ (from Ref. 22) define the effect of the inducer molecule IPTG on the Lac protein. Over a wide range of parameter values, the system has two stable fixed points; the null-clines are shown in Fig. 7(b).

The time courses of switching between stable states in the two models are shown in Fig. 8; transitions are induced by eliminating the bistability, then restoring it. The precise time course of switching from one stable state to another is determined by the way in which the model parameters are adjusted to eliminate the bistability. In each case, some parameter is increased until the system passes through a saddle
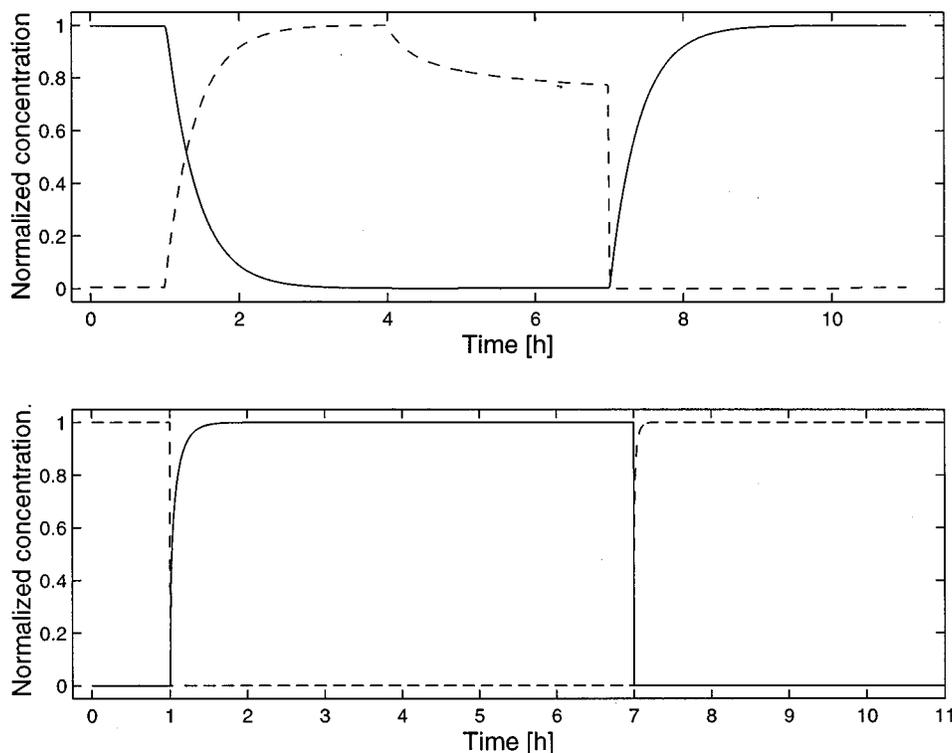
FIG. 8. Transitions between stable states for the two-protein bistable switch systems. The protein concentrations have been normalized (the trace for each protein is normalized relative to its own maximum value). The system parameters are varied over time, altering the stability of the system and causing transitions, as described in the text. Upper plots: The switching of Lac (solid) and CI (dashed) in the synthetic toggle model (Ref. 22). The parameter values are as given in the caption to Fig. 7, except as follows. (1–4 hours): [IPTG]=2 mM, $k=1.0$. (7–10 hours): [IPTG]=0.0, $k=53.5$. Lower plots: The switching of CRO (dashed line) and CI (solid) in the synthetic λ model. The parameter values are as given in the caption to Fig. 7, except as follows. (1–4 hours): $\gamma_x=0.004$, $\gamma_y=21.6$. (7–10 hours): $\gamma_x=18.0$, $\gamma_y=0.008$.

node bifurcation: two stable fixed points and one unstable fixed point collapse into a single stable point. In an effort to examine the behavior of the two systems under analogous conditions, we eliminate the bistability in every case by setting the system to a parameter value which is 50% past the bifurcation point; this factor was selected to correspond to the experimental IPTG-induced switching carried out in Ref. 22.

The transitions shown in Fig. 8 are generated as follows. The system begins (0–1 hour) in its default bistable state, sitting at one of the two stable fixed points. Then (1–4 hours) the bistability is eliminated (as described above), with the only remaining fixed point being such that the other protein has a high concentration. Once the concentrations have switched, the default parameters are restored and the system moves to the nearby stable fixed point (4–7 hours). Finally, the system is rendered monostable again (7–10 hours), causing another transition, followed by a period (10–11 hours) during which the bistable parameters are restored.

Under the conditions shown, the λ switch model displays significantly more rapid transitions between its stable states than those seen in the model of the toggle switch. The numerical results indicate that the properties of the λ switch do offer an advantage in terms of the speed of transitions, indicating that it may be fruitful to study synthetic models based on this natural system. Future analytical work on models such as the one presented in this section may allow us to

make more precise statements regarding the source of this advantage.

VIII. CONCLUSION

From an engineering perspective, the control of cellular function through the design and manipulation of gene regulatory networks is an intriguing possibility. Current examples of potential applicability range from the use of genetically engineered microorganisms for environmental cleanup purposes,[64] to the flipping of genetic switches in mammalian neuronal cells.[65] While the experimental techniques employed in studies of this nature are certainly impressive, it is clear that reliable theoretical tools would be of enormous value. On a strictly practical level, such techniques could potentially reduce the degree of ''trial-and-error'' experimentation. More importantly, computational and theoretical approaches will lead to testable predictions regarding the current understanding of complex biological networks.

While other studies have centered on certain aspects of naturally-occurring genetic regulatory networks,[9,12–14,18,24,25,38,39] an alternative approach is to focus on the design of synthetic networks. Such an engineering-based approach has significant technological implications, and will lead, in a complementary fashion, to an enhanced understanding of biological design principles. In this work, we have shown how several synthetic networks can be de-

signed from the genetic machinery of the virus λ phage. We have highlighted some of the possible behavior of these networks through the discussion of the design of two types of switches and a relaxation oscillator. Additionally, in the case of the oscillator, we have coupled the network to an existing cellular process. Such coupling could lead to possible strategies for entraining or inducing network oscillations in cellular protein levels, and prove useful in the design of networks that interact with cellular processes that require precise timing.

With regard to model formulation, there are several intriguing areas for further work. For one, the number of molecules governing the biochemistry of genetic networks is often relatively small, leading to interesting issues involving internal noise. Recent pivotal work[17,18,27] has led to a systematic modeling approach which utilizes a Monte Carlo-type simulation of the biochemical reactions.[66] While this approach is impressively complete, its complexity makes analysis nearly impossible. An alternative approach could entail the use of Langevin equations, whereby the effects of internal noise are incorporated into stochastic terms whose magnitudes are concentration-dependent. Indeed, in the context of genetic switches, this approach has recently been suggested.[67] The advantage of this formulation is that stochastic effects can be viewed as a perturbation to the deterministic picture, so that analytic tools can be utilized.

A potentially important technical issue involves the implicit assumption that the reactions take place in three-dimensional space. While this assumption is perhaps the most natural, proteins have been observed sliding along a DNA molecule in search of a promoter region,[68] so that protein–DNA reactions might effectively take place on a surface. While this would not alter the qualitative form of Eq. (6), the exponents on the variable x could take on other values,[69] and this, in turn, could lead to significant quantitative differences.

It has been nearly 30 years since the pioneering theoretical work on interacting genetic networks.[1–8] Due, in part, to the inherent complexity of regulatory networks, the true significance of these studies had to await technological advances. Current progress in the study of both naturally-occurring and synthetic genetic networks suggests that, as the pioneers envisioned, tools from nonlinear dynamics and statistical physics will play important roles in the description and manipulation of the dynamics underlying cellular control.

ACKNOWLEDGMENTS

[1] L. Glass and S. A. Kauffman, ''The logical analysis of continuous, non-linear biochemical control networks,'' J. Theor. Biol. **39**, 103 (1973).
[2] M. A. Savageau, ''Comparison of classical and autogenous systems of regulation in inducible operons,'' Nature (London) **252**, 546 (1974).
[3] S. Kauffman, ''The large-scale structure and dynamics of gene control circuits: An ensemble approach,'' J. Theor. Biol. **44**, 167 (1974).

[4] L. Glass, ''Classification of biological networks by their qualitative dynamics,'' J. Theor. Biol. **54**, 85 (1975).
[5] L. Glass, ''Combinatorical and topological methods in nonlinear chemical kinetics,'' J. Chem. Phys. **63**, 1325 (1975).
[6] M. Savageau, *Biochemical System Analysis* (Addison-Wesley, Reading, MA, 1976).
[7] B. C. Goodwin, *Analytical Physiology of Cells and Developing Organisms* (Academic, London, 1976).
[8] J. J. Tyson and H. G. Othmer, ''The dynamics of feedback control circuits in biochemical pathways,'' Prog. Theor. Biol. **5**, 1 (1978).
[9] G. K. Ackers, A. D. Johnson, and M. A. Shea, ''Quantitative model for gene regulation by λ phase repressor,'' Proc. Natl. Acad. Sci. U.S.A. **79**, 1129 (1982).
[10] B. O. Palsson and E. N. Lightfoot, ''Mathematical modeling of dynamics and control in metabolic networks,'' J. Theor. Biol. **113**, 279 (1985).
[11] F. Moran and A. Goldbeter, ''Onset of birhymicity in a regulated biochemical system,'' Biophys. Chem. **20**, 149 (1984).
[12] J. Reinitz and J. R. Vaisnys, ''Theoretical and experimental analysis of the phase lambda genetic switch implies missing levels of co-operativity,'' J. Theor. Biol. **145**, 295 (1990).
[13] B. Novak and J. J. Tyson, ''Modeling the control of DNA replication in fission yeast,'' Proc. Natl. Acad. Sci. U.S.A. **94**, 9147 (1997).
[14] B. Novak and J. J. Tyson, ''Quantitative analysis of a molecular model of mitotic control in fission yeast,'' J. Theor. Biol. **173**, 283 (1995).
[15] B. J. Hammond, ''Quantitative study of the control of HIV-1 gene expression,'' J. Theor. Biol. **163**, 199 (1993).
[16] A. Keller, ''Model genetic circuits encoding autoregulatory transcription factors,'' J. Theor. Biol. **172**, 169 (1995).
[17] H. H. McAdams and A. Arkin, ''Simulation of prokaryotic genetic circuits,'' Annu. Rev. Biophys. Biomol. Struct. **27**, 199 (1998).
[18] A. Arkin, J. Ross, and H. H. McAdams, ''Stochastic kinetic analysis of developmental pathway bifurcation in phage λ-infected *Escherichia coli* cells,'' Genetics **149**, 1633 (1998).
[19] P. Smolen, D. A. Baxter, and J. H. Byrne, ''Frequency selectivity, multistability, and oscillations emerge from models of genetic regulatory systems,'' Am. J. Physiol. **43**, C531 (1998).
[20] D. M. Wolf and F. H. Eeckman, ''On the relationship between genomic regulatory element organization and gene regulatory dynamics,'' J. Theor. Biol. **195**, 167 (1998).
[21] M. B. Elowitz and S. Leibler, ''A synthetic oscillatory network of transcriptional regulators,'' Nature (London) **403**, 335 (2000).
[22] T. S. Gardner, C. R. Cantor, and J. J. Collins, ''Construction of a genetic toggle switch in *Escherichia coli*,'' Nature (London) **403**, 339 (2000).
[23] A. Becksei and L. Serrano, ''Engineering stability in gene networks by autoregulation,'' Nature (London) **405**, 590 (2000).
[24] D. Endy, L. You, J. Yin, and I. J. Molineux, ''Computation, prediction, and experimental tests of fitness for bacteriophage T7 mutants with permuted genomes,'' Proc. Natl. Acad. Sci. U.S.A. **97**, 5375 (2000).
[25] A. Sveiczer, A. Csikasz-Nagy, B. Gyorffy, J. J. Tyson, and B. Novak, ''Modeling the fission yeast cell cycle: Quantized cycle times in $wee1^{-1}cdc25\Delta$ mutant cells,'' Proc. Natl. Acad. Sci. U.S.A. **97**, 7865 (2000).
[26] H. H. McAdams and L. Shapiro, ''Circuit simulation of genetic networks,'' Science **269**, 650 (1995).
[27] H. H. McAdams and A. Arkin, ''Stochastic mechanisms in gene expression,'' Proc. Natl. Acad. Sci. U.S.A. **94**, 814 (1997).
[28] L. H. Hartwell, J. J. Hopfield, S. Leibler, and A. W. Murray, ''From molecular to modular cell biology,'' Nature (London) **402**, C47 (1999).
[29] D. A. Lauffenburger, ''Cell signaling pathways as control modules: Complexity for simplicity?'' Proc. Natl. Acad. Sci. U.S.A. **97**, 5031 (2000).
[30] R. Weiss and T. F. Knight, ''Engineered communications for microbial robotics,'' *DNA6: 6th International Meeting on DNA Based Computers* (Leiden, The Netherlands, 2000).
[31] J. Monod, J. Wyman, and J. P. Changeux, ''On the nature of allosteric transitions: A plausible model,'' J. Mol. Biol. **12**, 88 (1965).
[32] A. Novick and M. Weiner, ''Enzyme induction as an all-or-none phenomenon,'' Proc. Natl. Acad. Sci. U.S.A. **43**, 553 (1957).
[33] W. Chen, P. Kallio, and J. E. Bailey, ''Construction and characterization of a novel cross-regulation system for regulating cloned gene expression in *Escherichia coli*,'' Genetics **130**, 15 (1993).
[34] D. Bray, ''Protein molecules as computational elements in living cells,'' Nature (London) **376**, 307 (1995).
[35] N. Barkai and S. Leibler, ''Biological rhythms: Circadian clocks limited by noise,'' Nature (London) **403**, 267 (2000).

[36] B. Lewin, *Genes VI* (Oxford University Press, Oxford, 1997).

[37] A more general treatment would incorporate all possible DNA-repressor binding configurations. However, the additional reactions have binding affinities characterized by equilibrium constants that are significantly smaller than for those considered, and their inclusion will not alter the general conclusions derived in this work.

[38] M. A. Shea and G. K. Akers, ''The O_R control system of bacteriophage lambda: A physical–chemical model for gene regulation,'' J. Mol. Biol. **181**, 211 (1985).

[39] P. Wong, S. Gladney, and J. D. Keasling, ''Mathematical model of the *lac* operon: Inducer exclusion, catabolite repression, and diauxic growth on glucose and lactose,'' Biotechnol. Prog. **13**, 132 (1997).

[40] W. R. McClure, ''Mechanism and control of transcription initiation in prokaryotes,'' Annu. Rev. Biochem. **54**, 171 (1985).

[41] P. H. von Hippel, ''An integrated model of the transcription complex in elongation, termination, and editing,'' Science **281**, 660 (1998).

[42] F. Jacob and J. Monod, ''Genetic regulatory mechanisms in the synthesis of proteins,'' J. Mol. Biol. **3**, 318 (1961).

[43] R. Dickson, J. Ableson, W. Barnes, and W. Reznikoff, ''Genetic regulation: The *lac* control region,'' Science **187**, 27 (1975).

[44] M. A. Savageau, ''Comparison of classical and autogenous systems of regulation in inducible operons,'' Nature (London) **252**, 546 (1974).

[45] J. Monod and F. Jacob, ''General conclusions: Teleonomic mechanisms in cellular metabolism, growth, and differentiation,'' Cold Spring Harbor Symp. Quant. Biol. **26**, 389 (1961).

[46] M. Ptaschne *et al.*, ''How the λ repressor and cro work,'' Cell **19**, 1 (1980).

[47] B. J. Meyer, R. Maurer, and M. Ptashne, ''Gene regulation at the right operator (O_R) of bacteriophage λ,'' J. Mol. Biol. **139**, 163 (1980).

[48] A. D. Johnson *et al.*, ''λ repressor and cro—Components of an efficient molecular switch,'' Nature (London) **294**, 217 (1981).

[49] A. D. Johnson, C. O. Pabo, and R. T. Sauer, ''Bacteriophage λ repressor and cro protein: Interactions with operator DNA,'' Methods Enzymol. **65**, 839 (1980).

[50] D. H. Ohlendorf and B. W. Matthews, ''Structural studies of protein–nucleic acid interactions,'' Annu. Rev. Biophys. Bioeng. **12**, 259 (1983).

[51] J. Hasty, D. McMillen, F. Isaacs, and J. J. Collins (in preparation).

[52] See other Focus Articles in this issue of Chaos.

[53] J. Sancho, M. S. Miguel, and S. Katz, Phys. Rev. A **26**, 1589 (1982).

[54] M. Samoilov, A. Arkin, and J. Ross, ''On the deduction of chemical reaction pathways from measurements of time series of concentrations,'' Chaos **11**, 108 (2001).

[55] W. Horsthemke and R. Lefever, *Noise-Induced Transitions* (Springer-Verlag, Berlin, 1984).

[56] J. Hasty, J. Pradines, M. Dolnik, and J. J. Collins, ''Noise-based switches and amplifiers for gene expression,'' Proc. Natl. Acad. Sci. U.S.A. **97**, 2075 (2000).

[57] N. G. Van Kampen, *Stochastic Processes in Physics and Chemistry* (North-Holland, Amsterdam, 1992).

[58] D. V. Rozanov, R. D'Ari, and S. P. Sineoky, ''RecA-independent pathways of lambdoid prophage induction I *Escherichia coli*,'' J. Bacteriol. **180**, 6306 (1998).

[59] M. Marek and I. Schrieber, *Chaotic Behavior of Deterministic Dissipative Systems* (Cambridge University Press, Cambridge, 1991).

[60] G. H. Hardy and E. M. Wright, in *An Introduction to the Theory of Numbers* (Clarendon, Oxford, 1979).

[61] M. Ptashne, *A Genetic Switch: Phage λ and Higher Organisms* (Cell, Cambridge, MA, 1992).

[62] A. Villaverde, A. Benito, E. Viaplana, and R. Cubarsi, ''Fine regulation of cI857-controlled gene expression in continuous culture of recombinant *Escherichia coli* by temperature,'' Appl. Env. Microbiol. **59**, 3485 (1993).

[63] H. B. Lowman and M. Bina, ''Temperature-mediated regulation and downstream inducible selection for controlling gene expression from the bacteriophage λ P_L promoter,'' Genetics **96**, 133 (1990).

[64] P. Szafranski *et al.*, ''A new approach for containment of microorganisms: Dual control of streptavidin expression by antisense RNA and the T7 transcription system,'' Proc. Natl. Acad. Sci. U.S.A. **94**, 1059 (1997).

[65] T. C. Harding *et al.*, ''Switching transgene expression in the brain using an adenoviral tetracycline-regulatable system,'' Nature Biotech. **16**, 553 (1998).

[66] D. Gillespie, ''Exact stochastic simulation of coupled chemical reactions,'' J. Phys. Chem. **81**, 2340 (1977).

[67] W. Bialek, ''Stability and noise in biochemical switches,'' cond-mat/0005235—Los Alamos Preprint Server, 2000.

[68] Y. Harada *et al.*, ''Single-molecule imaging of RNA polymerase–DNA interactions in real time,'' Biophys. J. **76**, 709 (1999).

[69] M. A. Savageau, ''Development of fractal kinetic theory for enzyme-catalysed reactions and implications for the design of biochemical pathways,'' BioSystems **47**, 9 (1998).